Journal of Catalysis 268 (2009) 89–99

Contents lists available at ScienceDirect

Journal of Catalysis

journal homepage: www.elsevier.com/locate/jcat

Rhenium complexes and clusters supported on γ-Al_2O_3: Effects of rhenium oxidation state and rhenium cluster size on catalytic activity for *n*-butane hydrogenolysis

Rodrigo J. Lobo-Lapidus, Bruce C. Gates *

Department of Chemical Engineering and Materials Science, University of California at Davis, One Shields Avenue, Davis, CA 95616, USA

ARTICLE INFO

Article history:
Received 13 July 2009
Revised 31 August 2009
Accepted 5 September 2009
Available online 7 October 2009

Keywords:
EXAFS spectroscopy
Supported rhenium clusters
Rhenium oxidation state
n-Butane hydrogenolysis

ABSTRACT

Supported metals prepared from $H_3Re_3(CO)_{12}$ on γ-Al_2O_3 were treated under conditions that led to various rhenium structures on the support and were tested as catalysts for *n*-butane conversion in the presence of H_2 in a flow reactor at 533 K and 1 atm. After use, two samples were characterized by X-ray absorption edge positions of approximately 5.6 eV (relative to rhenium metal), indicating that the rhenium was cationic and essentially in the same average oxidation state in each. But the Re–Re coordination numbers found by extended X-ray absorption fine structure spectroscopy (2.2 and 5.1) show that the clusters in the two samples were significantly different in average nuclearity despite their indistinguishable rhenium oxidation states. Spectra of a third sample after catalysis indicate approximately Re_3 clusters, on average, and an edge position of 4.5 eV. Thus, two samples contained clusters approximated as Re_3 (on the basis of the Re–Re coordination number), on average, with different average rhenium oxidation states. The data allow resolution of the effects of rhenium oxidation state and cluster size, both of which affect the catalytic activity; larger clusters and a greater degree of reduction lead to increased activity.

1. Introduction

Oxidation states of the metals in transition metal complex catalysts influence the bonding and reactivity of ligands and thereby the catalytic properties of the complexes [1]. The oxidation states of metals in solid catalysts exert similar influences, but they are difficult to determine, because the metal species engaged in catalysis are often minority surface species, and the metal may be present in more than one oxidation state, making the characterization of the active species challenging. Typical supported metal catalysts consist of dispersed particles that are large enough to have metallic character [2], but as the particles become smaller, approaching nanometers in diameter, they are more strongly influenced by the support and more likely to bear positive charges, with the corresponding changes in their catalytic properties. Metal atoms at metal–support interfaces have been suggested to be positively charged even when the metals are noble [3], including gold [4].

There is a long history of attempts to separate effects of metal particle size and metal oxidation state in catalysis by supported metals, but for the most part such a resolution has been difficult [5], in part because it is difficult to determine these properties in supported metal catalysts that incorporate particles that are nonuniform in size and structure [6].

Group-7 metals form stable cationic clusters in solution [7] and on oxide surfaces [8], and they are good candidates for the preparation of supported clusters in which the metals are cationic and present in oxidation states that depend on the treatment conditions. Among the group-7 metals, rhenium is appealing because it offers examples of molecular clusters of a given nuclearity with the metal in different oxidation states [7,9] and because it forms highly stable cationic clusters on surfaces exemplified by γ-Al_2O_3 [8,10].

Our goals were to investigate rhenium on γ-Al_2O_3, attempting to produce extremely small clusters of various sizes incorporating the metal in various oxidation states and to distinguish the effects of cluster size and metal oxidation state on catalysis; the catalytic reaction was chosen to be *n*-butane hydrogenolysis, a structure-sensitive reaction that is important in the technology of hydrocarbon conversion [11].

Treatment with H_2 of samples formed from $H_3Re_3(CO)_{12}$ supported on γ-Al_2O_3 has been shown to lead to the formation of relatively well-defined cationic rhenium clusters [8,10]; the treatment also removes the CO ligands from the metal frame, which Kirlin et al. [12] showed to be strong inhibitors of cyclopropane conversion.

* Corresponding author. Fax: +1 530 752 1031.
E-mail address: bcgates@ucdavis.edu (B.C. Gates).

0021-9517/$ - see front matter © 2009 Elsevier Inc. All rights reserved.
doi:10.1016/j.jcat.2009.09.006

2. Experimental

2.1. Synthesis

2.1.1. Synthesis of $H_3Re_3(CO)_{12}$

Synthesis of $H_3Re_3(CO)_{12}$ was carried out by the method of Andrews et al. [13]. Tetrahydrofuran (99+%, Sigma–Aldrich) was purified by refluxing over sodium. Cyclohexane (99%, EM Science) and phosphoric acid (85%, Fisher) were degassed by sparging of N_2. $Re_2(CO)_{10}$ (Pressure Chemicals) and $NaBH_4$ (98+%, Acros) were used as received. All handling during the syntheses was carried out with Schlenk techniques to minimize exposure to air. The $H_3Re_3(CO)_{12}$ was purified by recrystallization in cyclohexane and was stored in an argon-filled glove box until it was used for the synthesis of the supported catalysts.

2.1.2. $H_3Re_3(CO)_{12}$ supported on γ-Al_2O_3

Inside the glove box, the support, γ-Al_2O_3 (Degussa, Alu C) powder, which had been treated at 773 K in flowing O_2 for 4 h then under vacuum for 16 h, and the precursor, $H_3Re_3(CO)_{12}$, were placed into a flask and sealed with a rubber stopper. *n*-Pentane (>99%, Fisher) (purified by sparging of N_2 and dried by passage though a column containing particles of 3A molecular sieve) was transferred to the flask with a double-tip cannula and slurried with $H_3Re_3(CO)_{12}$ and γ-Al_2O_3 for 24 h. The mixture was then evacuated for 24 h to remove the *n*-pentane. The resultant sample was transferred to the glove box with exclusion of air and moisture and was stored until used.

2.2. Sample treatment and catalyst testing

Treatment of samples and their testing as catalysts were carried out with a once-though quartz tubular flow reactor. The powder sample was held in place with a quartz frit mounted near the center of the reactor, which was held in an electrically heated tube furnace. The temperature was measured in the reactor below the frit with a k-type thermocouple. Loading of the samples into the reactor was done inside the argon-filled glove box. The reactor was sealed on both ends with O-ring compression fittings to exclude air and moisture, both before and after use. For catalyst testing, a 500-mg sample was mixed with 3.5 g of inert, nonporous α-Al_2O_3 particles (Fisher) and was placed in the reactor downstream of a bed of 4.5 g of α-Al_2O_3 particles. Samples of the catalyst that were to be characterized later by X-ray absorption spectroscopy (XAS) were treated in the reactor and subjected to catalytic reaction conditions as stated above, but in the absence of α-Al_2O_3. After catalysis these samples, still in the reactor, were flushed with flowing helium and then transferred back to the argon-filled glove box and handled in an inert atmosphere until their characterization.

2.2.1. Sample treatment

To obtain decarbonylated clusters on the support, samples formed by adsorption of $H_3Re_3(CO)_{12}$ on γ-Al_2O_3 were treated in flowing H_2 at 773 K for 2 h (Sample A, Table 1). This treatment has been found to produce cationic trirhenium clusters on γ-Al_2O_3 [8,10]. Fractions of this sample were further treated for 2 h with a stream of helium containing O_2 at a partial pressure of 10 kPa, at 423 K (Sample B, Table 1). Fractions of sample B were then treated under reducing conditions, flowing H_2 at 773 K for 2 h, giving Sample C (Table 1); such a treatment has been shown to produce aggregates of rhenium dispersed on the support when the precursor was ReO_4^- [8]. All treatments were carried out at atmospheric pressure (101 kPa).

2.2.2. Catalyst testing: conversion of n-butane

The catalytic conversion of *n*-butane was carried out at 533 K and 101 kPa; the partial pressure of *n*-butane was 14.5 kPa, with the balance being H_2, and the total feed flow rate was 4.08×10^{-3} mol/s (100 ml/min at room temperature and 179 ml/min under reaction conditions).

Samples of the effluent gas were analyzed every 25 min with an on-line gas chromatograph equipped with an FID detector and a Plot-Al_2O_3 column. Conversions were differential (<5%), determining reaction rates directly. Calculation of turnover frequencies (TOFs) was based on the assumptions that (a) the reactor was a plug-flow reactor and (b) all the Re atoms were accessible to reactants and active. Selectivity for each of the products was calculated as the mass ratio of the product formed to the *n*-butane converted. The errors in the TOF and selectivities were calculated by propagating the errors from the following sources: masses of the catalyst, determined both during sample preparation and loading of the reactor; gas flow rates; errors in the GC peak areas; pressure; and temperature.

The samples resulting from the use of samples A, B, and C for the catalytic conversion of *n*-butane for approximately 36 h in the flow reactor are referred to as samples A′, B′, and C′, respectively (Table 1). A fraction of Sample B was treated in H_2 at 533 K for 36 h, giving Sample D.

The sample notation is summarized in Table 1.

2.3. Characterization of catalysts

2.3.1. Infrared (IR) spectroscopy

IR characterization was done with a Bruker 90v/s instrument equipped with a DTGS detector and a HgCdTe detector. Samples in the glove box were pressed between KBr windows and placed in a gas-tight cell (International Crystal Laboratories). Each sample was then scanned under vacuum (1 mbar) with a spectral resolution of 2 cm^{-1}; a minimum of 128 scans was recorded per sample.

2.3.2. XAS

2.3.2.1. Data collection. X-ray absorption fine structure (XAFS) spectra were collected at beam line 10-2 at the Stanford Synchrotron Radiation Laboratory (SSRL) at the Stanford Linear Accelerator Center and at beam line X-18B at the National Synchrotron Light Source (NSLS) at Brookhaven National Laboratory. The beam en-

Table 1
Sample designations.

Sample name	Conditions of treatment of sample prepared from $H_3Re_3(CO)_{12}$ supported on γ-Al_2O_3
A	Flowing H_2 for 2 h at 773 K
B	Flowing H_2 for 2 h at 773 K followed by flowing O_2 for 2 h at 423 K
C	Flowing H_2 for 2 h at 773 K followed by flowing O_2 for 2 h at 423 K followed by flowing H_2 for 2 h at 773 K
A′	Flowing H_2 for 2 h at 773 K followed by use as a catalyst for *n*-butane conversion for 36 h
B′	Flowing H_2 for 2 h at 773 K followed by flowing O_2 for 2 h at 423 K followed by use as a catalyst for *n*-butane conversion for 36 h
C′	Flowing H_2 for 2 h at 773 K followed by flowing O_2 for 2 h at 423 K followed by flowing H_2 for 2 h at 773 K followed by use as a catalyst for *n*-butane conversion for 36 h
D	Flowing H_2 for 2 h at 773 K followed by flowing O_2 for 2 h at 423 K followed by flowing H_2 for 36 h at 533 K

ergy was selected by means of a double-crystal monochromator, a Si (2 2 0) crystal with a minimum step size of 0.35 eV at SSRL, and a Si (1 1 1) crystal with a minimum step size of 0.4 eV at NSLS. The dimensions of the X-ray beam were in all cases approximately 1×12 mm. To reduce the presence of higher-energy harmonics in the beam, the monochromator was detuned to 70%. The samples were scanned in transmission mode with gas-filled ion chambers used to measure the intensity of the X-rays entering and exiting the sample. Furthermore, a reference foil (rhenium at SSRL and hafnium at NSLS) was scanned simultaneously with the sample to allow calibration of the energy scale.

Samples in a nitrogen-filled glove box were pressed into self-supporting wafers and loaded into the cell, which allowed scanning without exposure to air or moisture and under high vacuum ($<2 \times 10^{-5}$ mbar) and at 77 K [14].

XAFS spectra in the XANES region were determined by scanning at the smallest step size possible (0.35 eV at SSRL and 0.4 eV at NSLS), whereas in the EXAFS region the samples were scanned with a step size of 0.07 k (k is the wave vector), corresponding to a total scan time of 15 min. Each reported spectrum is an average of at least four spectra.

2.3.2.2. XANES data analysis. Data in the XANES region were processed and analyzed by using the software package Athena [15]. The edge position of the rhenium in the sample was taken as the first inflection point in the XAFS spectrum. To accurately determine the edge shift of the sample, the energy scale of the XAFS spectrum was calibrated by setting the edge position of the metal foil to the reported value. Then a minimum of two spectra were averaged.

To allow a comparison between spectra of different samples, the XANES spectra were normalized to account for the different sample thicknesses. This normalization procedure is described elsewhere [15].

2.3.2.3. EXAFS data reduction and analysis. Data reduction and analysis were carried out with the software package XDAP [16]. First, a minimum of four scans were aligned and then averaged to improve data quality and extend the range of data that could be analyzed. Analysis of the data was performed by using a difference file technique; the functions used to construct the structural models and used to minimize the error are shown elsewhere [17]. The fitting was done in k-space and in R-space by using three k-weightings (typically k, k^2, and k^3). For a model to be considered appropriate, it was required to fit well with all k-weightings. In the fitting, the number of fitted parameters (four per shell) did not exceed the number of statistically justified parameters, as determined by the Nyquist theorem [18].

Fit quality of each model was evaluated by the value of $(\Delta\chi)^2$, as defined by the International XAFS Society [19]. This parameter takes into account the number of fitted parameters and statistically independent data points, thus allowing the comparison of models containing different numbers of contributions and different fit ranges. By using $(\Delta\chi)^2$ we were able to determine whether the addition of each new contribution to an EXAFS model improved the fit.

Two criteria were used to determine whether an EXAFS fit was valid: (1) that the addition of each of the shells to the model resulted in a reduction of the value of $(\Delta\chi)^2$ and (2) that the parameters for each shell were physically appropriate, specifically, in terms of distances; furthermore, the value of ΔE_0 was considered appropriate only if $-10 \text{ eV} < \Delta E_0 < 10 \text{ eV}$; and the value of $\Delta\sigma^2$ was considered appropriate only if the magnitude was $0 < \Delta\sigma^2 < 1.5 \times 10^{-2}$ Å^{-2}. Discrimination between valid models representing the same data set was carried out on the basis of the $(\Delta\chi)^2$ parameter; the model with the lowest values was preferred.

Amplitude- and phase-shift functions for each of the contributions were calculated with the software FEFF7 [20]. The input for the calculations was obtained from crystallographic data; Table 5 shows the reference compounds used in the calculations.

The value of the amplitude reduction factor S_0^2 used for the data analysis was 0.92. This was determined by fitting data characterizing $H_3Re_3(CO)_{12}$ mixed with boron nitride.

3. Results

3.1. Formation of samples containing rhenium clusters of various sizes

IR spectra of samples formed by the adsorption of $H_3Re_3(CO)_{12}$ on γ-Al_2O_3, before and after treatment in flowing H_2 at 773 K (Sample A), show that the clusters were completely decarbonylated during the treatment (Supplementary material). This result is bolstered by the absence of a multiple-scattering Re–O contribution in the EXAFS results characterizing this sample (Table 2). Furthermore, the EXAFS data show that the Re–Re contribution was essentially the same before and after the treatment, with the coordination number being approximately 2, consistent with the inference that the trirhenium framework of the precursor $H_3Re_3(CO)_{12}$ remained intact. Hence, we infer that decarbonylated Re_3 clusters

Table 2
EXAFS parameters for best-fit models representing samples prepared from $H_3Re_3(CO)_{12}$ supported on γ-Al_2O_3.[a]

Sample name	Absorber–backscatterer pair	N[e]	R (Å)[e]	$\Delta\sigma^2 \times 10^{-3}$ (Å^{-2})[e]	ΔE_0 (eV)[e]	$(\Delta\chi)^2$ [f]
A[a,b] [10]	Re–Re	2.1 ± 0.1	2.65 ± 0.00	7.4 ± 0.3	−0.9 ± 0.6	25.3
	Re–O	0.9 ± 0.0	2.01 ± 0.00	0.2 ± 0.2	−0.9 ± 0.6	
	Re–O	0.6 ± 0.0	2.48 ± 0.01	0.5 ± 0.5	−8.8 ± 0.8	
B[a,c]	Re–O	1.3 ± 0.1	2.00 ± 0.01	2.3 ± 0.6	9.0 ± 0.8	2.1
	Re–O	2.1 ± 0.1	2.50 ± 0.02	8.0 ± 1.3	1.4 ± 0.8	
	Re–O	1.9 ± 0.0	1.72 ± 0.00	1.4 ± 0.4	−3.9 ± 0.2	
C[a,d]	Re–Re	4.7 ± 0.0	2.72 ± 0.00	7.2 ± 0.1	−3.8 ± 0.1	28.4
	Re–O	0.8 ± 0.0	2.01 ± 0.00	0.1 ± 0.1	−9.5 ± 0.2	
	Re–O	1.0 ± 0.0	2.41 ± 0.01	2.8 ± 0.6	8.7 ± 0.4	

[a] Treatments stated in Section 2.
[b] k-Range: 4.3–13.7 Å^{-1}.
[c] k-Range: 3.5–13.6 Å^{-1}.
[d] k-Range: 2.4–14.3 Å^{-1}.
[e] Errors shown correspond to precisions in the EXAFS fit; the estimated accuracies are as follows: for low-Z backscatterers: N, ±20%; R, ±0.04 Å; $\Delta\sigma^2$, ±20%; ΔE_0, ±20%; for high-Z backscatterers: N, ±10%; R, ±0.02 Å; $\Delta\sigma^2$, ±20%; ΔE_0, ±20%.
[f] $(\Delta\chi)^2$ is a measure of the quality of the fit, as defined elsewhere [19].

were bonded to the support after decarbonylation. These results are consistent with earlier observations with similar samples [8,10].

EXAFS spectra characterizing Sample B give no evidence of Re–Re contributions (Table 2); thus we infer that O_2 treatment led to cluster fragmentation and the formation of mononuclear rhenium species. These EXAFS data are consistent with those obtained for γ-Al_2O_3-supported samples prepared from methyltrioxorhenium, showing the presence of Re–O contributions at 1.72 Å and at approximately 2.00 Å [21]. The latter distance matches that of typical metal–$O_{support}$ contributions for a variety of metals and supports [22], consistent with the inference that the mononuclear rhenium species were bonded to the γ-Al_2O_3.

EXAFS data characterizing Sample C show the presence of a Re–Re contribution with a coordination number of 4.5 (Table 2), corresponding, on average, to clusters of about 10 atoms each (assuming a hemispherical model of the clusters and hcp packing). Thus, treatment of the initially site-isolated mononuclear rhenium species in flowing H_2 led to the formation of larger clusters than those present initially. This result nearly matches that of Fung et al. [8], who treated and characterized a sample prepared from NH_4ReO_4 supported on γ-Al_2O_3. This comparison suggests that the species formed by fragmentation of the Re_3 frame underwent aggregation more or less in the same way as the species formed from Fung's perrhenate precursor. The EXAFS parameters characterizing these samples are similar to each other, but, within error, not the same (Table 2); we lack sufficient information to interpret the differences.

The three forms of the supported samples made from $H_3Re_3(CO)_{12}$ were characterized by X-ray absorption edge shifts (relative to rhenium metal) which indicate that the rhenium in each sample was cationic (Table 3). The edge shift values show that the rhenium in the sample containing the mononuclear species (Sample B; characterized by a Re–O contribution at 1.72 Å) was present in a higher oxidation state than the rhenium in the other samples before their use as catalysts; the least oxidized rhenium was observed in the sample containing the larger clusters; it was characterized by the smallest edge shift (among the samples characterized before catalytic testing), relative to that of rhenium metal (Table 3).

Table 3
Edge shift values characterizing the Re L_{III} edge of the samples prepared from $H_3Re_3(CO)_{12}$ supported on γ-Al_2O_3 before and after use as catalysts in the conversion of *n*-butane.

Sample name	Edge shift (eV)[a]	Ref.
A	5.0 ± 0.4	[11]
B	4.5 ± 0.4	This work
C	6.9 ± 0.4	This work
A′	4.5 ± 0.4	This work
B′	5.6 ± 0.4	This work
C′	5.8 ± 0.4	This work

[a] Edge shift relative to that of metallic rhenium (10,535 eV). Errors correspond to the minimum energy grid size for each of the synchrotrons.

3.2. Catalytic performance of samples with various rhenium cluster sizes

3.2.1. Cluster size affects catalytic properties for the conversion of *n*-butane

The sample incorporating clusters approximated as Re_3 (Sample A) was tested as a catalyst for *n*-butane conversion, as were the samples incorporating mononuclear rhenium species (Sample B) and larger rhenium clusters (Sample C). The catalytic activity of each sample as a function of time on stream (TOS) is shown in Fig. 1.

During the 36 h of testing in the flow reactor, Sample C was consistently the most active of the three catalysts. During the first five hours of operation, the activity of this catalyst (measured

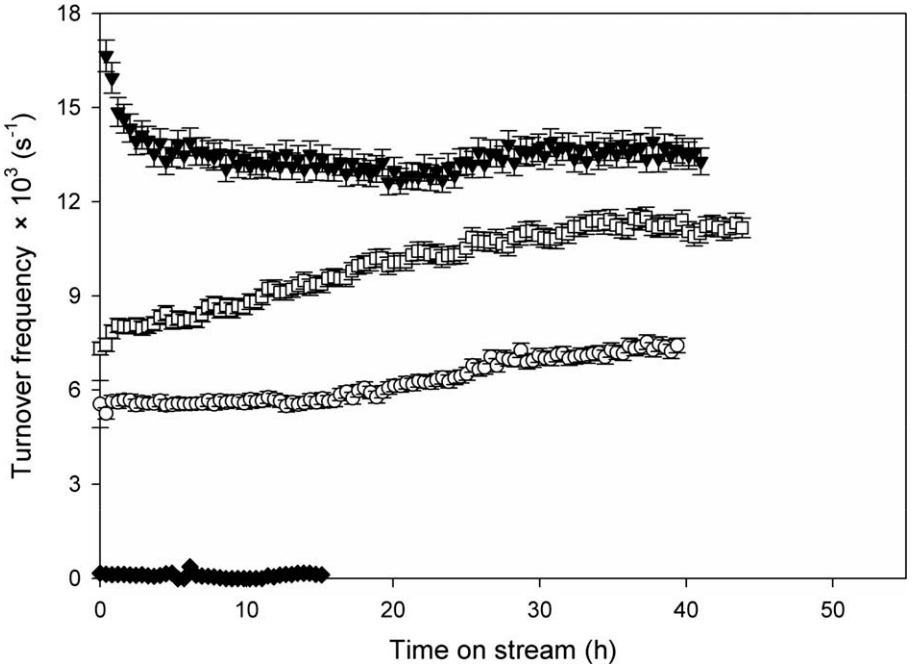

Fig. 1. Catalytic activities of samples containing supported rhenium species of various sizes: (□) sample initially containing clusters approximated as Re_3 (Sample A); (○) sample initially containing mononuclear rhenium species (Sample B); (▼) sample initially containing larger rhenium clusters (Sample C); (♦) sample containing only γ-Al_2O_3 (no Re) (for comparison, the TOF calculation was performed by arbitrarily assuming that the number of active sites was equal to that in 500 mg of the catalyst containing 1 wt% Re).

by the TOF) decreased from $(1.66 \pm 0.05) \times 10^{-2}\ s^{-1}$ to $(1.38 \pm 0.04) \times 10^{-2}\ s^{-1}$, thereafter remaining essentially unchanged.

Sample A was characterized by an initial TOF of $(7.3 \pm 0.2) \times 10^{-3}\ s^{-1}$; the activity increased with time on stream, to a value of $(1.12 \pm 0.03) \times 10^{-2}\ s^{-1}$ after approximately 36 h, when the run was stopped. Sample B was the one with the lowest catalytic activity (with a TOF value of $(7.4 \pm 0.2) \times 10^{-3}\ s^{-1}$ when the reaction was stopped); however, the activity of this sample also increased during operation (Fig. 1).

3.2.2. Influence of rhenium cluster size on product distribution in n-butane conversion catalysis

The products of *n*-butane conversion were methane, ethane, propane, and propylene; product distribution data are shown in Fig. 2. In all cases, the principal product was methane, indicating that the dominant reaction was hydrogenolysis. Sample C was the catalyst with the highest selectivity for methane (Fig. 2C); for example, the methane selectivity at the end of the run was 65.1 ± 1.2 wt%. Sample A was characterized by a selectivity for methane of 60.1 ± 0.5 wt% (Fig. 2A). Sample B was characterized by a methane formation selectivity of 57.8 ± 1.2 wt% (Fig. 2B). The selectivity for methane (and the other products) of Sample C did not change, within error, with TOS. Methane selectivity of Sample A increased during the first 3 h of the experiment and then slowly decayed until the experiment was stopped. In contrast, the methane selectivity of sample B was characterized by an initial period of rapid decay (5 h), followed by a slower monotonic decay for the remainder of the experiment.

Formation of ethane and propane as products of *n*-butane conversion, which constitute the second and third most abundant products with each of the catalysts, provides evidence beyond that provided by the formation of methane of the occurrence of hydrogenolysis as the dominant reaction. Sample A (the catalyst initially containing clusters approximated as Re_3) was more selective for ethane than the other samples; the catalyst with the lowest selectivity for ethane was Sample C. The catalyst with the highest selectivity for propane formation was Sample B, and the least selective was Sample A.

Propylene was observed as a product with each of the catalysts, but the selectivities were low: 1.3, 1.7, and 1.9 wt% for Samples A, B, and C, respectively. These results show that the catalysts had some activity for dehydrogenation or (more likely) cracking of *n*-butane (the cracking reaction would be expected to have led to the formation of methane and propylene).

3.3. Structural changes of catalysts resulting from operation

3.3.1. EXAFS evidence of changes in the environment of clusters approximated as Re_3 without significant changes in cluster nuclearity

EXAFS data characterizing Sample A′ (Fig. 5, which before catalysis contained clusters approximated as Re_3), give no evidence of any change, within error (the overall error bound is taken to include the sum of the bounds in the precision and the accuracy—for each EXAFS model), of the cluster nuclearity, as shown by the Re–Re coordination number (Table 4). This result is consistent with earlier observations of the lack of change in the cluster nuclearity after the use of the sample as a catalyst for methylcyclohexane conversion at 723 K [10], in contrast to the changes in the Re–Re distance observed after the latter conversion; the data representative of sample A′ indicate no significant change in the corresponding distance ($R = 2.64$ Å) (see Table 5).

Nonetheless, there were detectable changes in the EXAFS data resulting from exposure of the sample to catalytic reaction conditions. The coordination number of the Re–O contribution at a relatively short distance (1.98 Å)—associated with bonding of rhenium to the support—decreased from 0.9 before catalysis to 0.3 after catalysis; the Re–O distance characterizing this contribution remained unchanged, within error. The coordination number characterizing the longer Re–O contribution, however, increased from 0.6 to 1.2 during catalysis; thus, the overall Re–O coordination number remained constant, within the error of the EXAFS models (which includes both the precision and the accuracy). Simultaneously, the distance characterizing the latter contribution decreased from 2.48 Å initially to 2.39 Å after catalysis. This change is an indication that the rhenium–support interaction became stronger as catalysis took place. In summary, the data show that although the use of the sample containing the clusters approximated as Re_3 did not lead to a change the average cluster nuclearity, it did lead to a change in the environment surrounding the clusters.

3.3.2. Retention of average cluster size in sample incorporating larger rhenium clusters during catalysis of n-butane conversion

EXAFS parameters characterizing Sample C′ (Table 4; plots in Supplementary material) indicate that the Re–Re coordination number (5.1) remained the same—within the error of the EXAFS fits (including both accuracy and precision)—as that in the sample before use as a catalyst (Sample C). Although the cluster size remained essentially unchanged during catalysis, the longer Re–O contribution changed markedly, being characterized by a significantly increased coordination number (Tables 2 and 4).

These results are contrasted with the usual pattern observed with supported group-8 metal clusters, whereby an increase in the metal–oxygen coordination number is usually accompanied by fragmentation of the clusters, leading to a lower metal–metal coordination number [23].

3.3.3. Formation of clusters from mononuclear rhenium species under catalytic reaction conditions and in H_2

When Sample B was used as a catalyst for 36 h at 533 K (producing Sample B′), rhenium clusters formed, as shown by a Re–Re shell with a distance of 2.72 Å that was not present in the spectrum of unused Sample B. The corresponding coordination number was 2.3, which matches (within error) that of Sample A′, inferred to contain Re_3 clusters, on average. This comparison indicates that clusters that can be approximated as trirhenium, on average, formed during catalysis and were stable. The difference in Re–Re distances characterizing Samples A′ and B′ suggests that the clusters in Sample A′ are characterized by stronger Re–Re bonds.

Prior to catalysis, Sample B was characterized by a Re–O contribution at 1.72 Å (Table 4), but, after catalysis, this contribution was no longer detectable. Moreover, the coordination number of the Re–O shell at 2.00 Å decreased from 1.3 to 0.8 after catalysis. The changes in the Re–Re and Re–O shells are consistent with the typical behavior of supported group-8 metals [23], whereby cluster formation is accompanied by a decrease in the number of M–O bonds. As for the sample containing the larger clusters, the Re–Re distance representative of this sample is similar to that in metallic rhenium.

Similarly, treatment of the sample initially containing mononuclear rhenium species (Sample B) in flowing H_2 for 36 h at 533 K led to the appearance of a Re–Re contribution. As for the sample used as a catalyst, the Re–O contribution at 1.72 Å disappeared, and the coordination number of the Re–O contribution at 2.00 Å decreased slightly (Table 4). The clusters in Sample D are inferred to have been larger, on average, than those formed during catalysis, as the corresponding Re–Re coordination number (4.1) is significantly greater than that characterizing the used catalyst (2.3). This result suggests that the absence of *n*-butane in the H_2 treatment and/or (more likely) the higher H_2 partial pressure applied when H_2 was used alone led to an increase in the rate of cluster formation and/or growth.

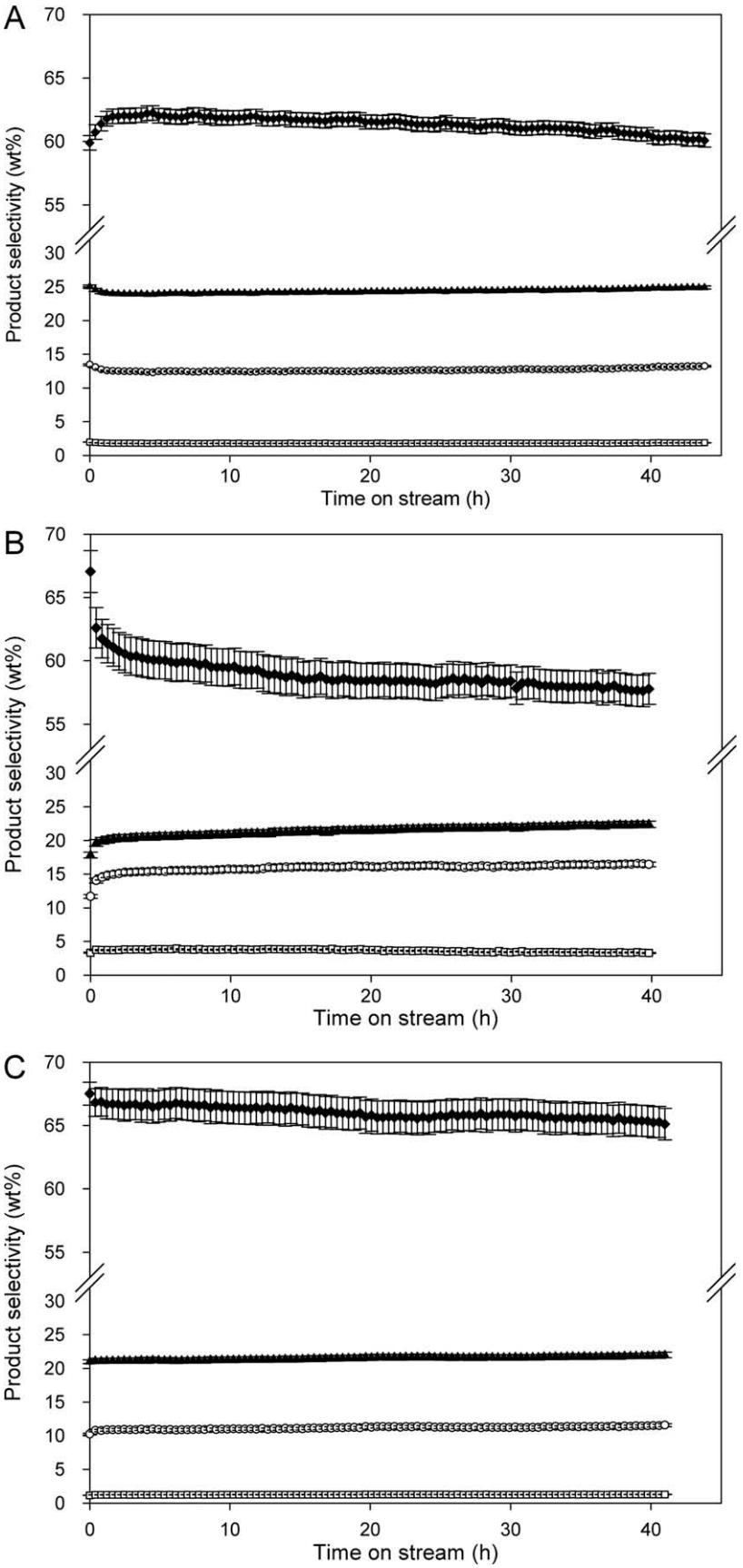

Fig. 2. Selectivity data characterizing each of the catalyst samples during the conversion of *n*-butane at 533 K: (A) sample initially containing clusters approximated as Re_3 (Sample A); (B) sample initially containing mononuclear Re species (Sample B); (C) sample initially containing larger rhenium clusters (Sample C). Selectivities are shown for methane (♦), ethane (▲), propane (○), and propylene (□).

Table 4
EXAFS parameters characterizing best-fit models representing samples formed from $H_3Re_3(CO)_{12}$ supported on γ-Al_2O_3 after use for *n*-butane conversion or treatment in H_2.[a]

Sample name	Absorber–backscatterer pair	N[f]	R (Å)[f]	$\Delta\sigma^2 \times 10^{-3}$ (Å^{-2})[f]	ΔE_0 (eV)[f]	$(\Delta\chi)^2$[g]
A′[a,b]	Re–Re	2.4 ± 0.1	2.64 ± 0.00	8.7 ± 0.7	0.3 ± 2.2	45.1
	Re–O	0.3 ± 0.1	1.98 ± 0.00	3.7 ± 0.8	0.3 ± 2.2	
	Re–O	1.2 ± 0.2	2.39 ± 0.00	6.3 ± 0.7	7.6 ± 0.7	
B′[a,c]	Re–Re	2.2 ± 0.1	2.72 ± 0.00	5.3 ± 0.5	−3.5 ± 0.2	31.1
	Re–O	0.8 ± 0.0	2.04 ± 0.00	−0.3 ± 0.5	−9.7 ± 0.2	
	Re–O	2.5 ± 0.0	2.47 ± 0.00	6.8 ± 0.7	0.9 ± 0.2	
C′[a,d]	Re–Re	5.1 ± 0.1	2.73 ± 0.00	6.7 ± 2.0	−4.0 ± 0.1	67.3
	Re–O	0.9 ± 0.0	2.02 ± 0.00	0.6 ± 0.5	−8.5 ± 0.2	
	Re–O	1.4 ± 0.0	2.46 ± 0.01	7.1 ± 0.7	1.5 ± 0.3	
D[a,e]	Re–Re	3.9 ± 0.1	2.73 ± 0.00	6.4 ± 0.2	−4.7 ± 0.3	26.1
	Re–O	1.1 ± 0.0	2.02 ± 0.00	1.0 ± 0.4	−9.2 ± 0.2	
	Re–O	2.8 ± 0.1	2.47 ± 0.01	9.5 ± 0.4	−0.2 ± 0.7	
	Re–O	1.9 ± 0.3	3.25 ± 0.02	6.0 ± 0.8	7.4 ± 1.6	

[a] Treatments stated in Section 2.
[b] *k*-Range: 2.4–13.2 Å^{-1}.
[c] *k*-Range: 2.3–13.5 Å^{-1}.
[d] *k*-Range: 2.4–13.4 Å^{-1}.
[e] *k*-Range: 2.4–13.5 Å^{-1}.
[f] Errors shown correspond to precisions in the EXAFS fit; the estimated accuracies are as follows: for low-Z backscatterers: N, ±20%; R, ±0.04 Å; $\Delta\sigma^2$, ±20%; ΔE_0, ±20%; for high-Z backscatterers: N, ±10%; R, ±0.02 Å; $\Delta\sigma^2$, ±20%; ΔE_0, ±20%.
[g] $(\Delta\chi)^2$ is a measure of the quality of the fit, as defined elsewhere [19].

Table 5
Reference compounds used for the calculation of EXAFS amplitude and phase-shift functions.

Compound	Absorber–backscatterer pair	N	R (Å)
ReAl [29]	Re–Al	8	2.49
$Re_3(O\text{–}i\text{-}Pr)_9$[a] [7]	Re–O_s	2	1.91
ReO_2 [29]	Re–O_l	2	2.11
Rhenium metal [29]	Re–Re	12	2.74

[a] O–*i*-Pr represents isopropoxide.

3.3.4. Evidence of changes in environment of Re_3 species without changes in rhenium oxidation state

The XAFS edge shift characterizing Sample A′ (Table 3) matches, within error, that of the sample before use as a catalyst (Sample A), a result that indicates that the rhenium did not undergo a significant change in oxidation state as a result of its exposure to catalytic reaction conditions. XANES spectra characterizing Samples A and A′ (Fig. 3) show a significant increase in the white-line intensity after use, symptomatic of changes in the coordination environment of the Re atoms. This qualitative information is in accord with the EXAFS results showing significant changes in the Re–O contributions. Notwithstanding the changes in the coordination environment, there was no detectable change in formal oxidation state of the rhenium—as shown directly by the edge position (Table 3) and indirectly by the sum of coordination numbers representing all the Re–O contributions (Table 4).

3.3.5. Aggregation accompanied by partial reduction of mononuclear rhenium species on the support

A comparison of the edge position shift (Table 3) characterizing Sample B′ relative to that of Sample B indicates that the rhenium underwent reduction during catalysis, consistent with its aggregation to form small clusters as demonstrated by the appearance of a Re–Re contribution in the EXAFS spectra and the decrease in the Re–O contributions (Table 4). Notwithstanding this reduction, the edge shift characterizing the used catalyst (5.8 eV, Table 3) indicates that the rhenium remained cationic. Furthermore, the larger edge shift indicated by the spectrum of this sample relative to that of Sample A′, which contained clusters of roughly the same average size (4.5 eV, Table 3), shows that the rhenium in the clusters formed from Sample B was more highly oxidized than the rhenium in Sample A′. XANES spectra of Sample B′ (Fig. 4) show there was a large decrease in the white-line intensity and of the edge position characterizing Sample B as it was used for the conversion of *n*-butane (thereby being transformed into Sample B′). Such changes are consistent with the changes in the environment surrounding the rhenium species, specifically, the growth of rhenium clusters and the reduction of the rhenium as well as a decrease in the number of Re–O contributions, as demonstrated by the EXAFS data (Table 4).

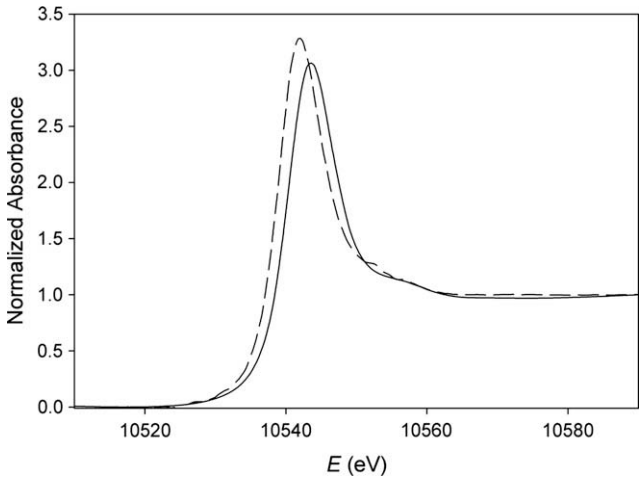

Fig. 3. XANES spectra characterizing the sample initially containing clusters approximated as Re_3, before (—; Sample A) and after (– – –; Sample A′) use as a catalyst for the conversion of *n*-butane. Each spectrum was calibrated relative to the reference metal (rhenium or hafnium; see text) that was scanned simultaneously.

Furthermore, the differences in white-line intensity characterizing Samples B′ and D suggest that the presence of *n*-butane in the treatment gas and/or the change in H_2 partial pressure affected the nature of the clusters, consistent with the EXAFS data (Table 4) showing that the average rhenium clusters were much larger in the latter sample.

3.3.6. Oxidation of larger rhenium clusters under catalytic reaction conditions shown by XANES

The edge shift of Sample C′ relative to that of Sample C (Table 3) indicates that the clusters were oxidized under catalytic reaction

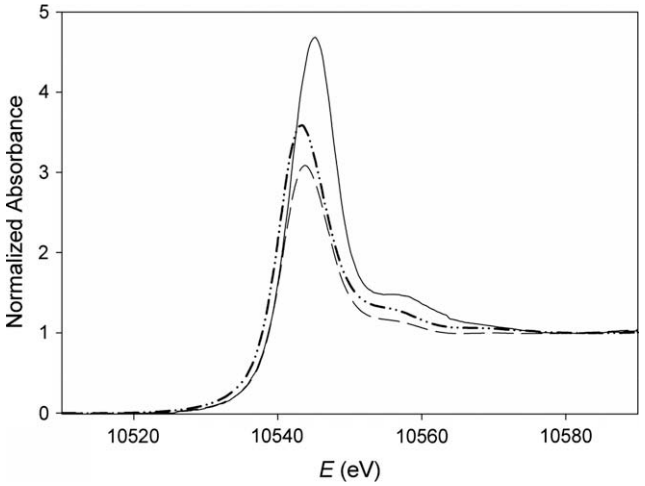

Fig. 4. XANES characterizing the sample initially containing mononuclear rhenium species; before (—; Sample B) and after (– – –; Sample B′) use as a catalyst [spectra are calibrated relative to the reference metal (rhenium or hafnium; see text) that was scanned simultaneously]; and after treatment at 533 K for 36 h in flowing H_2 (– · · –; Sample D). (The energy scale representing the spectra of the sample initially containing mononuclear species after 36 h under H_2 flow at 533 K was not calibrated; thus, the shift indicated in the plot is arbitrary.)

conditions, with the edge shift increasing from 4.5 eV for the latter to 5.6 eV for the former. The edge shift of Sample C′ matches within error that of Sample B′ (formed from mononuclear species), a result that suggests that rhenium in similar oxidation states was present in these samples containing clusters of markedly different average sizes.

4. Discussion

4.1. Reducibility of rhenium on γ-Al_2O_3

The data provide evidence of the resistance of supported rhenium clusters to reduction to the zerovalent form, consistent with the observations reported [24] for supported samples prepared from perrhenate precursors; the latter samples required temperatures exceeding 773 K to convert the rhenium into a metallic form. The results are consistent with the oxophilic nature of rhenium, and they are contrasted with observations of supported noble metals, which readily form zerovalent aggregates when subjected to reducing conditions, even at temperatures as low as 373 K, for example, for the formation of clusters from zeolite-supported rhodium complexes [25]. Supported complexes of noble metals can even be reduced (autoreduced) in the absence of added reducing agents at low temperatures, as exemplified by the formation of supported gold clusters on TiO_2 from mononuclear species bonded to the support [26].

Thus, the supported rhenium samples offer the benefits of retention of high dispersions during catalysis at high temperatures. The resistance of rhenium to reduction may explain in part why it is used with group-8 metals in industrial catalysts, such as in the RePt catalysts used for naphtha reforming [27].

4.2. Control of rhenium cluster size and oxidation state

The results presented here indicate that the samples tested as catalysts for *n*-butane hydrogenolysis, a classic structure-sensitive reaction [11], contained extremely small rhenium clusters, with the rhenium being cationic. Two of our samples, A′ and B′, were found to contain clusters of similar average size, approximated as Re_3 (on the basis of EXAFS data), but to incorporate rhenium in significantly different average oxidation states, as indicated by the XAFS edge positions. The sample in which the rhenium in the final form was in the higher average oxidation state (Sample B′) is the one that, before being subjected to catalytic reaction conditions, contained mononuclear rhenium species, whereas the sample in which the rhenium was in a lower average oxidation state—but still cationic—was the one that contained clusters approximated

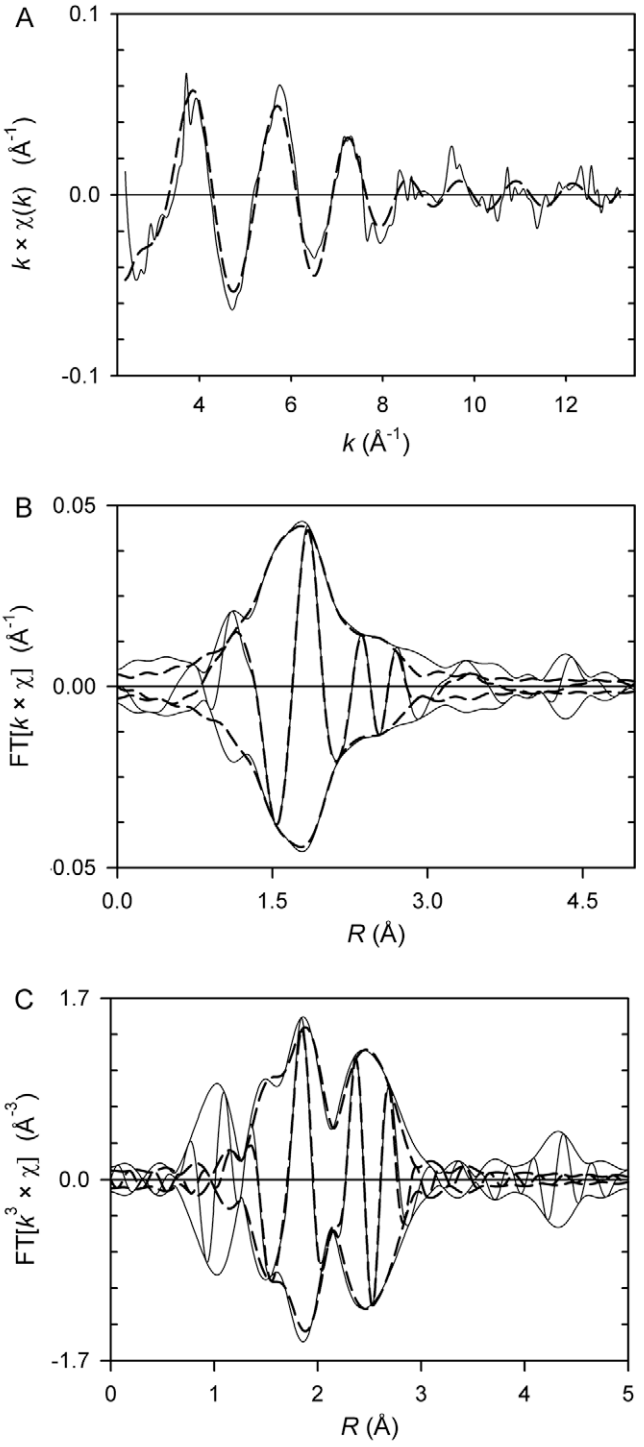

Fig. 5. EXAFS data characterizing supported Sample containing clusters approximated as Re_3 after use as a catalyst for the conversion of *n*-butane, Sample A′ (data, —; best-fit model, – – –): (A) k^1-weighted EXAFS function in *k*-space; (B) imaginary part and magnitude of k^1-weighted EXAFS function in *R*-space; and (C) imaginary part and magnitude of k^3-weighted EXAFS function in *R*-space.

as Re_3 before and after use as a catalyst (Samples A and A′). As a catalyst for the conversion of *n*-butane, the latter was more than 50% more active (at the end of the catalytic reaction test) than the former.

Moreover, the former sample—and a third sample, Sample C′ (incorporating more than about 10 Re atoms per cluster, on average)—incorporated rhenium in oxidation states that were indistinguishable from each other after the catalysts had been used for approximately 36 h, although the average cluster sizes in these samples were significantly different from each other (Table 4), as were their catalytic activities (Fig. 1). Sample B′ was found to have the lowest catalytic activity of any of the supported rhenium catalysts reported here.

After catalysis, the sample containing the larger clusters (Sample C′) was inferred to incorporate rhenium in clusters with roughly the same average nuclearity as in the sample before catalysis (as shown by the indistinguishable Re–Re coordination numbers), and this sample was characterized by the highest catalytic activity of any tested in this work.

These results demonstrate effects of the reaction environment on the catalyst structure and activity and provide a basis for deconvolution of the effects of rhenium cluster size and oxidation state on the activity. Thus, supported group-7 metals such as rhenium provide a significant opportunity to separate the effects of metal cluster size and metal oxidation state in catalysis.

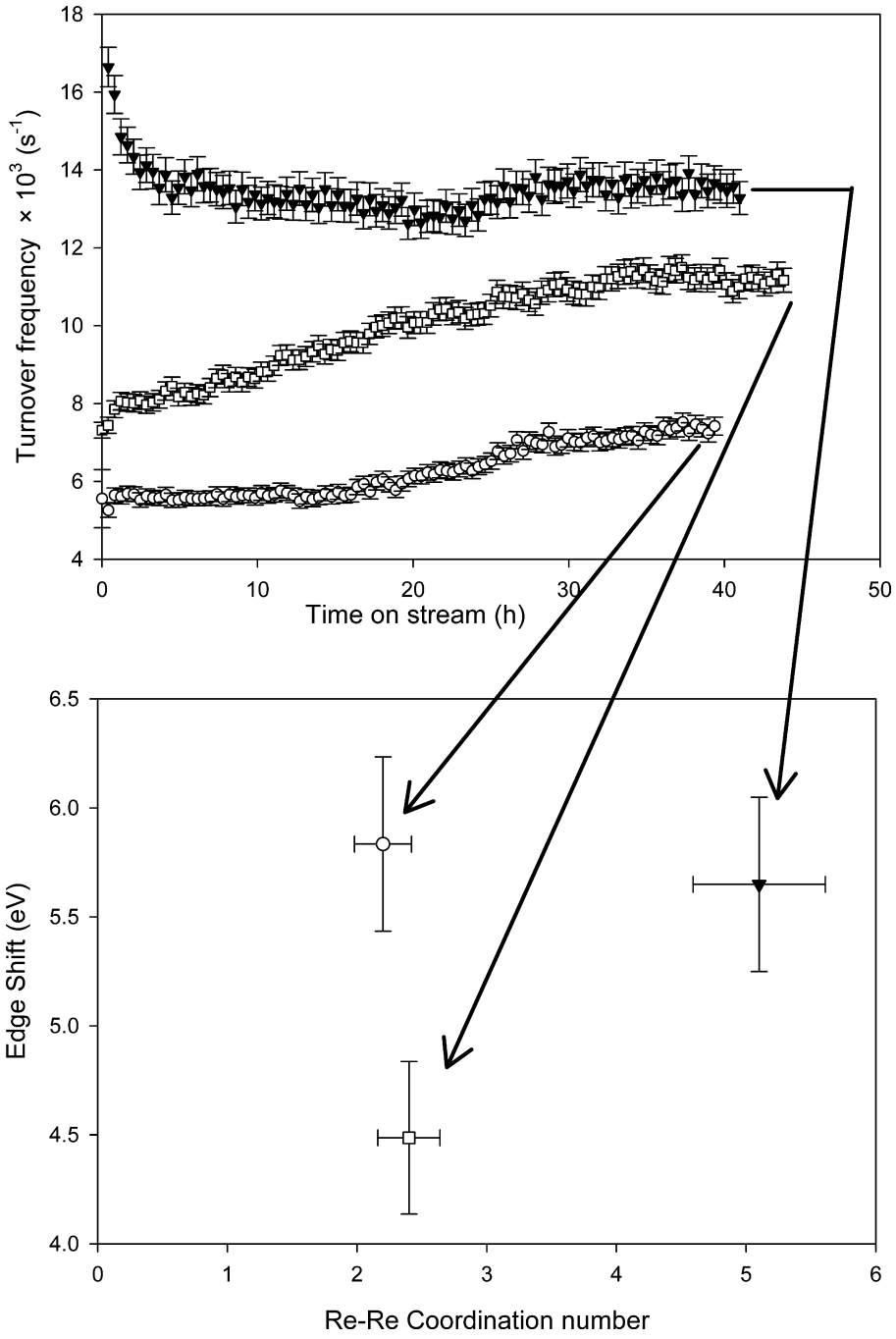

Fig. 6. Relationship between catalytic activity and XAS parameters indicative of cluster size and degree of oxidation of rhenium for each of the samples: (□) sample initially containing clusters approximated as Re_3 (Sample A′); (○) sample initially containing mononuclear rhenium species (Sample B′); and (▼) sample initially containing larger rhenium clusters (Sample C′).

The formation and growth of clusters in the sample initially containing mononuclear rhenium species (Sample B) under catalytic reaction conditions is contrasted with the lack of cluster growth in the samples initially containing clusters approximated as Re_3 (Sample A, formed directly by decarbonylation of the sample formed from $H_3Re_3(CO)_{12}$ supported on γ-Al_2O_3)—these are the samples showing the greatest resistance to reduction of any we tested.

Fung et al. [8] observed behavior consistent with that reported here, but they did not report any evidence of the structures of the rhenium species after catalysis or any comparison between their clusters formed from $H_3Re_3(CO)_{12}$ and clusters originating from mononuclear precursors made from $H_3Re_3(CO)_{12}$.

The behavior of the larger rhenium clusters under highly reductive catalytic reaction conditions when the clusters became oxidized as the reaction proceeded without any significant change in average apparent cluster size (as shown by the Re–Re coordination number) is contrasted with that of group-8 metals, for which oxidation is not expected to occur in a H_2-rich atmosphere and for which oxidation is typically accompanied by cluster fragmentation [28].

4.3. Resolution of effects of rhenium cluster size and rhenium oxidation state on catalytic activity

4.3.1. Influence of rhenium cluster size on catalytic activity for n-butane hydrogenolysis

As stated above, the EXAFS data show that the average rhenium cluster sizes in two samples, B′ and C′, were significantly different from each other; thus, because the rhenium oxidation states were nearly the same and the catalytic activities differed significantly, we infer that the differences in activity should be attributed primarily to the differences in average cluster size. The data indicate that the activity increases as the cluster size increases, at least in the size range of our experiments. The relationship is shown schematically in Fig. 6.

This inference agrees qualitatively with observations made with catalysts incorporating larger particles of group-8 metals; for example, increases in the average size of ruthenium particles led to increased activity for hydrogenolysis of cyclohexane [11]. There were no measurements of the ruthenium oxidation states in those samples, but the authors inferred that the particles were metallic.

4.3.2. Influence of rhenium oxidation state on catalytic activity for n-butane hydrogenolysis

Similarly, the XAFS edge positions characterizing two of the used samples, A′ and B′, indicate that the rhenium was in different oxidation states, although the average cluster sizes were essentially the same; thus, we attribute the significant difference in catalytic activity to the effect of the rhenium oxidation state. The greater catalytic activity for *n*-butane hydrogenolysis is attributed to the more highly reduced rhenium. We might suggest that the higher electron density in the rhenium frame might lead to a stronger bonding of the reactants to the catalytic sites and a more efficient activation of the adsorbed reactants in the more highly reduced catalyst; calculations at the density functional level would be helpful in testing this suggestion.

4.3.3. Dynamic behavior of catalysts explained by influence of rhenium cluster size and oxidation state

Although no structural information characterizing the catalysts in intermediate stages of the catalytic testing are available, the changes in the activity of the various samples can be explained by taking into account the effects of cluster size and oxidation state. As Sample C was tested, the catalytic activity decreased, concomitant with an increase in the degree of oxidation of rhenium (without a significant change in average cluster size), consistent with the inference stated above that more reduced clusters are more active and that as the clusters become oxidized the catalytic activity decays.

When Sample B was tested, the cluster size increased as did the degree of reduction of the rhenium; both effects are consistent with the increase in activity of this sample.

In summary, the data support the inference that both the size of the metal clusters and the oxidation state of the metal significantly influence the catalytic properties of supported rhenium for *n*-butane conversion.

5. Conclusions

The data provide evidence of the catalytic activity of nearly uniform γ-Al_2O_3-supported rhenium clusters prepared by the reduction of mononuclear rhenium species and by decarbonylation of a sample prepared from $H_3Re_3(CO)_{12}$. The oxidation state of rhenium in clusters formed from the mononuclear species depends on the treatment conditions rather than the initial size of the rhenium species. The characterization of a family of catalysts shows that the metal oxidation state and the average size of the metal cluster each affects the catalytic activity and selectivity; activity and selectivity for methane formation increase with increasing cluster nuclearity, and there is a separate effect of increasing catalytic activity and increasing methane selectivity with increasing reduction of the rhenium.

Acknowledgments

We thank Dr. Simon Bare of UOP LLC for helpful comments. This research was supported by the US Department of Energy, Office of Energy Research, Basic Energy Sciences, Contract FG02-87ER15600. Some of the work was carried out at the Stanford Synchrotron Radiation Laboratory (SSRL) and some at the National Synchrotron Light Source (NSLS). The SSRL is a national user facility operated by Stanford University on behalf of the US Department of Energy (DOE), Office of Science, Basic Energy Sciences. The SSRL Structural Molecular Biology Program is supported by the Department of Energy, Office of Biological and Environmental Research, and by the National Institutes of Health, National Center for Research Resources, Biomedical Technology Program. The NSLS is supported by the US Department of Energy, Office of Science, Basic Energy Sciences, under Contract No. DE-AC02-98CH10886; beam line X18-B is supported by the NSLS, through the Divisions of Materials and Chemical Sciences of the DOE, and the Synchrotron Catalysis Consortium (DE-FG02-05ER15688). We thank the beam line staffs for their assistance.

Appendix A. Supplementary material

Supplementary data associated with this article can be found, in the online version, at doi:10.1016/j.jcat.2009.09.006.

References

[1] D.F. Shriver, P.W. Atkins, Inorganic Chemistry, Oxford University Press, New York, 1999.
[2] B. Heinrichs, F. Noville, J.P. Pirard, J. Catal. 170 (1997) 366.
[3] G.N. Vayssilov, B.C. Gates, N. Rösch, Angew. Chem. 42 (2003) 1391.
[4] M. Haruta, in: B. Corain, G. Schmid, N. Toshima (Eds.), Metal Nanoclusters in Catalysis and Materials Science: The Issue of Size Control, Elsevier BV, Amsterdam, 2008, p. 183.
[5] M. Boudart, G. Djéga-Mariadassou, Kinetics of Heterogeneous Catalytic Reactions, Princeton University Press, Princeton, 1984. p. 173.
[6] J. Okal, W. Tylus, L. Kepinski, J. Catal. 225 (2004) 498.
[7] D.M. Hoffman, D. Lappas, D.A. Wierda, J. Am. Chem. Soc. 111 (1989) 1531.

[8] A.S. Fung, P.A. Tooley, M.J. Kelley, D.C. Koningsberger, B.C. Gates, J. Phys. Chem. 95 (1991) 2259.
[9] N. Masciocchi, A. Sironi, G. D'Alfonso, J. Am. Chem. Soc. 112 (1990) 9395.
[10] R.J. Lobo-Lapidus, M.J. McCall, M. Lanuza, S. Tonnesen, S.R. Bare, B.C. Gates, J. Phys. Chem. C 112 (2008) 3383.
[11] Y.L. Lam, J.H. Sinfelt, J. Catal. 42 (1976) 319.
[12] (a) P.S. Kirlin, B.C. Gates, Nature 325 (1987) 38;
(b) P.S. Kirlin, F.A. DeThomas, J.W. Bailey, H.S. Gold, C. Dybowski, B.C. Gates, J. Phys. Chem. 90 (1986) 4882;
(c) P.S. Kirlin, H. Knözinger, B.C. Gates, J. Phys. Chem. 94 (1990) 8451.
[13] M.A. Andrews, S.W. Kirtley, H.D. Kaesz, Inorg. Synth. 17 (1977) 66.
[14] R.E. Jentoft, S.E. Deutsch, B.C. Gates, Rev. Sci. Instrum. 67 (1996) 2111.
[15] B. Ravel, M. Newville, J. Synchrotron. Rad. 12 (2005) 537.
[16] M. Vaarkamp, J.C. Linders, D.C. Koningsberger, Physica B 209 (1995) 159.
[17] D.C. Koningsberger, B.L. Mojet, G.E. Dorssena, D.E. Ramaker, Top. Catal. 10 (2000) 143.
[18] E.A. Stern, Phys. Rev. B 48 (1993) 9825.
[19] International XAFS Society, "Error Reporting Recommendations: A Report of the Standards and Criteria Committee." http://www.i-x-s.org/OLD/subcommittee_reports/sc/err-rep.pdf (accessed June, 2009).
[20] J.J. Rehr, R.C. Albers, Rev. Mod. Phys. (2000) 621.
[21] N. Viswanadham, T. Shido, T. Sasaki, Y. Iwasawa, J. Phys. Chem. B 106 (2002) 10955.
[22] J. Guzman, B.C. Gates, J. Chem. Soc., Dalton Trans. (2003) 3303.
[23] S.E. Deutsch, J.T. Miller, K. Tomishige, Y. Iwasawa, W.A. Weber, B.C. Gates, J. Phys. Chem. 100 (1996) 13408.
[24] H.C. Yao, M. Shelef, J. Catal. 44 (1976) 392.
[25] A.J. Liang, B.C. Gates, J. Phys. Chem. C 112 (2008) 18039.
[26] J.C. Fierro-Gonzalez, B.C. Gates, J. Phys. Chem. B 109 (2005) 7275.
[27] J.H. Sinfelt, in: G. Ertl, H. Knözinger, J. Weitkamp (Eds.), Handbook of Heterogeneous Catalysis, VCH, Weinheim, 1997, p. 1939.
[28] J.G.C. Shen, A.M. Liu, T. Tanaka, M. Ichikawa, J. Phys. Chem. B 102 (1998) 7782.
[29] D.L. Calvert, P. Villars, W.B. Pearson, Pearson's Handbook of Crystallographic Data for Intermetallic Phases, American Society for Metals, Metals Park, 1985.